Original Article

The feasibility of superparamagnetic iron oxide–enhanced magnetic resonance imaging for assessing liver lesions in patients with contraindications for iodine CT contrast media or gadolinium-based MR contrast media: a retrospective case-control study

Chishio Kurata[1], Kazuhiro Saito[1], Natsuhiko Shirota[1], Yoichi Araki[1], Katsutoshi Sugimoto[2], Yu Tajima[1], Daisuke Yunaiyama[1]

[1]Department of Radiology, Tokyo Medical University, Tokyo, Japan; [2]Department of Gastroenterology and Hepatology, Tokyo Medical University, Tokyo, Japan

Contributions: (I) Conception and design: C Kurata, K Saito; (II) Administrative support: Y Araki, D Yunaiyama; (III) Provision of study materials or patients: K Sugimoto; (IV) Collection and assembly of data: N Shirota, Y Tajima, Y Araki; (V) Data analysis and interpretation: K Saito, Y Tajima; (VI) Manuscript writing: All authors; (VII) Final approval of manuscript: All authors.

Correspondence to: Kazuhiro Saito. Department of Radiology, Tokyo Medical University, 6-7-1, Nishi-Shinjuku, Shinjuku-ku, Tokyo 160-0023, Japan. Email: saito-k@tokyo-med.ac.jp.

Background: The detection and characterization of liver lesions are problematic in patients with bronchial asthma, renal dysfunction, or a history of allergy to gadolinium-based magnetic resonance contrast media or iodine-computed tomography contrast media because these contrast media cannot be used. Hence, the information on the lesion vascularity cannot be obtained. Therefore, this retrospective case-control study evaluated the feasibility of superparamagnetic iron oxide (SPIO) in patients with one or more of these contraindications who underwent SPIO-enhanced magnetic resonance imaging for the assessment of liver lesions.

Methods: Twenty-six patients with a total of 48 lesions were analyzed. SPIO was used in the case of all patients because each patient had at least one reason not to use iodine contrast or gadolinium-based contrast media. Additionally, all patients were subjected to the perfusion study. A total volume of 1.3 mL of SPIO was injected via the cubital vein at a rate of 3 mL per second, followed by 40 mL saline at the same speed. The scanning of the perfusion study was started 4 s after the beginning of superparamagnetic iron oxide injection and scanning took 50 s. Two radiologists independently evaluated whether the lesion was malignant or benign. Receiver operating characteristic analysis (ROC) was performed to determine the additional benefit of the perfusion study.

Results: There were no adverse effects associated with SPIO. The area under the curve (AUC) value without perfusion study for observers 1 and 2 were 0.473 (P=0.794, 95% CI: 0.275–0.672) and 0.602 (P=0.305, 95% CI: 0.407–0.798), respectively, whereas the Az values with perfusion study for observers 1 and 2 were 0.782 (P=0.011, 95% CI: 0.565–0.998) and 0.784 (P=0.004, 95% CI: 0.591–0.977), respectively. Az value became significantly better when the perfusion study has added (P=0.001 and 0.012 by observers 1 and 2).

Conclusions: SPIO can be used safely in patients with bronchial asthma, renal dysfunction, or a history of contrast media allergy. Furthermore, the diagnostic accuracy of SPIO was acceptable.

Keywords: Superparamagnetic iron oxide (SPIO); hepatocellular carcinoma; lesion vascularity; renal dysfunction; asthma

Submitted Jan 24, 2022. Accepted for publication Jun 15, 2022.
doi: 10.21037/qims-22-74
View this article at: https://dx.doi.org/10.21037/qims-22-74

Introduction

The significance of magnetic resonance imaging (MRI) for the detection and characterization of liver lesions has been widely accepted ever since hepatocyte-specific contrast media became available (1-3). However, patients with asthma, renal dysfunction, or severe allergic reactions to hepatocyte-specific contrast media cannot benefit from these technical advantages. For most of these patients, often contrast-enhanced CT cannot be used (4-6). When contrast media is not available, plain CT or MRI is used to evaluate the lesion; however, these techniques have limitations in both the detection and characterization of the lesions.

Superparamagnetic iron oxide (SPIO, Resovist®, FUJIFILM Toyama Chemical Co., Ltd., Japan) was widely used before the availability of hepatocyte-specific MRI contrast agents. In particular, it was used to differentiate arterial portal shunts or pseudo-lesions from neoplastic lesions. Although the number of countries where SPIO is available has decreased in recent years, its use in the detection of liver lesions has been reported to be as good as or better than that of dynamic CT (7-10). SPIO can be used safely in asthma patients. In addition, since SPIO is metabolized according to normal iron metabolism and does not affect renal dysfunction, it can also be used in patients with renal dysfunction. However, it has been reported that the diagnostic accuracy for hepatocellular carcinoma (HCC) is improved by adding diffusion-weighted images (DWI) to the SPIO-enhanced MRI (11). However, SPIO is sometimes taken up by well-differentiated HCC, including early-stage HCC (12), and it may not be possible to detect these lesions using either SPIO-enhanced MRI or diffusion-weighted imaging (12). In such cases, the evaluation of tumor blood flow is a significant clue to decide the therapeutic strategy. We have previously evaluated the blood flow of HCC or hepatocellular nodules by SPIO and reported its effectiveness (13-15). On the other hand, the better or equal detection of the metastatic lesion with SPIO-enhanced MRI has been reported than with enhanced CT or enhanced MR using nonspecific extracellular contrast media (10,16-18). It has also been reported that SPIO-enhanced MRI plus diffusion-weighted imaging provides even better diagnostic performance of liver metastasis than contrast-enhanced CT (19).

Here, we retrospectively evaluated the feasibility of SPIO for patients who, because of bronchial asthma, renal dysfunction, or a history of contrast media allergy, could not be analyzed with hepatocyte-specific contrast media, non-specific extracellular MR contrast media, or iodine CT contrast media. We present the following article in accordance with the STROBE reporting checklist (available at https://qims.amegroups.com/article/view/10.21037/qims-22-74/rc).

Methods

Ethical approval

This study was conducted in accordance with the Declaration of Helsinki (as revised in 2013). The institutional ethics review board of Tokyo Medical University (No. T2020-0339) approved this retrospective case-control study and individual consent for this retrospective analysis was waived.

Subjects

By searching the radiology reporting system, the subjects were selected from a group of 537 patients who underwent SPIO-enhanced MRI between January 1, 2008, and December 31, 2020. The exclusion criteria were as follows; 1. Not performing perfusion study, 2. Absence of contraindications of contrast media such as a history of bronchial asthma, renal dysfunction, and a history of adverse reaction by Gd-based contrast media or iodinated contrast media, 3. Without a final diagnosis of the liver lesion or determination of the absence of the lesion (*Figure 1*). Out of a total of 537 patients, 500 patients were not administered SPIO rapidly, and dynamic imaging was not acquired. The remnant 37 patients were administered SPIO rapidly, and dynamic imaging was acquired, namely in the perfusion study. Further, 11 of 37 patients were excluded because the SPIO-enhanced MRI was not due to contraindication of Gd-based and iodinated contrast media, or no final diagnosis of the liver lesion. Finally, these subjects consisted of 26 patients (18 men and eight women), and their mean age was 73 years old (20–92 years). Concerning the purpose of the examination, 17 patients were evaluated for recurrence

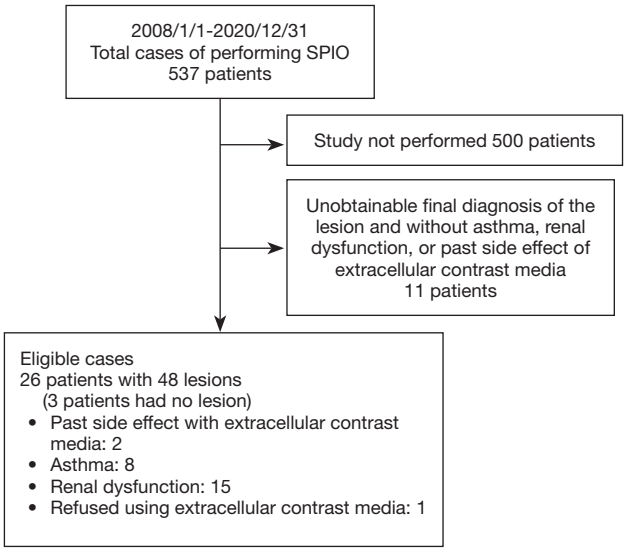

Figure 1 Participant selection flowchart.

Table 1 Background of patients and lesion characteristics

Background of patients and lesion characteristics	Numbers of patients or lesions
Underlying disease	
Hepatitis B	5
Hepatitis C	9
Hepatitis B and C	1
Nonalcoholic steatohepatitis	1
Alcoholism	1
Colorectal cancer	3
Pancreatic cancer	2
Nothing particular	4
Contraindication	
Asthma	8
History of side effects with Gd-based contrast media	2
Renal dysfunction (KDIGO)	
G3a	3
G3b	5
G4	3
G5	5
Liver lesion	
HCC	10
Metastatic tumor	4
Focal nodular hyperplasia	1
HCC post treatment (without recurrence)	24
Metastatic tumor post treatment (without recurrence)	1
Cyst	2

KDIGO, Kidney Disease Improving Global Outcomes; HCC, hepatocellular carcinoma.

after HCC treatment, two for evaluation of the presence or absence of HCC in hepatitis type C, five for detection of metastatic liver tumors, and two for the characterization of liver lesions. The underlying diseases were five cases of hepatitis type B, nine of hepatitis type C, one of both hepatitis type B and C, one of nonalcoholic steatohepatitis, one of alcoholism, three of colorectal cancer, two of pancreatic cancer, and four for nothing in particular (*Table 1*). A definitive diagnosis of the liver lesion was made by biopsy, surgery, angiography-assisted CT, contrast-enhanced US, or the observation of clinical course. The lesions that showed no change or a decreased size by the plain CT or SPIO-enhanced MRI after six months or more, and no enhancement by the contrast-enhanced US, were clinically diagnosed as therapeutically approachable lesions or benign lesions. On the other hand, the lesions were diagnosed as HCC if viral hepatitis was detected, enhancement on contrast-enhanced US or hypervascularity on CT hepatic arteriography were found, and there was evidence of corona enhancement in its delayed phase.

MRI acquisition

A superconductive 1.5 Tesla MR system (Avanto, Siemens, Germany) was used. Pre-contrast MRI included T1-weighted images (in and opposed phase) and T2-weighted images. As previously reported, a total volume of 1.3-mL SPIO (36.2-mg Fe) was injected via the cubital vein at a rate of 3 mL per second, followed by 40-mL saline at the same speed (14,15). The scanning of perfusion study was started at 4 s after the beginning of SPIO injection, scanning took 50 s, and a hundred phases were obtained. Enhanced T1-weighted images that were short TE were obtained 3 min after the injection of SPIO, whereas T2-weighted images and T2*-weighted images were obtained 10 min after SPIO injection. The details of the imaging sequences are described in *Table 2*.

Table 2 Parameters of each MRI sequence

	T1WI	T2WI	Heavy T2WI	T1WI short TE	T2* WI	DWI	Perfusion study
Pre-contrast	A	A	A	N/A	N/A	A	N/A
Post-contrast	N/A	A	N/A	A	A	N/A	A
Breath-holding	Breath-holding	Breath-holding	Breath-holding	Breath-holding	Breath-holding	Free Breathing	Breath-holding
TR/TE	6.7/2.39, 4.77	3,000/91	1,000/111	3.4/1.27	130/9	4,800/73	460/20
Flip angle	15°	150°	120°	12°	30°, 60°		90°
Matrix	320×60	384×70	256×100	384×72	352×80	160×100	192×81
Slice thickness	2 mm	5 mm	5 mm	2 mm	5 mm	5 mm	8 mm
Slice gap	0	1 mm	1 mm	0	1 mm	1 mm	1.6 mm
Averaging	1	1	1	1	1	b=0, 200, 3 averages, b =800, 5 averages	1
Acquisition time	15 s	36 s	42 s	21 s	50 s	2 min 24 s	50 s
Algorithm	PAT factor 4 with CAIPIRINHA	PAT factor 2 with GRAPPA	PAT factor 2 with GRAPPA	PAT factor 3 with CAIPIRINHA	PAT factor 2 with GRAPPA	PAT factor 2 with GRAPPA	PAT factor 2 with GRAPPA
Notes	–	Echo train length, 5; 2 concatenations	Turbo factor, 176; 2 concatenations		2 concatenations	b values 0, 200, 800 sec/mm^2; EPI factor, 132	EPI factor 156; measurements 100 times

WI, weighted image; DWI, diffusion-weighted image; A, applicable; N/A, not applicable; PAT, parallel acquisition technique; CAIPIRINHA, controlled aliasing in parallel imaging results in higher acceleration; GRAPPA, generalized autocalibrating partially parallel acquisitions; EPI, echo planar image.

Analysis

A certified radiologist with more than 30 years of experience diagnosed each lesion based on the images and clinical information. Since some cases had multiple liver lesions; a maximum of three lesions were evaluated per patient. We first focused on the suspected or definite malignant lesions because the goal was to detect the lesions that required therapy. Therefore, when three or more malignant lesions were present, the largest three lesions were selected. In cases with malignant and benign lesions, malignant lesions were first selected, and then, if fewer than three malignant lesions were found, benign nodules were also included, starting from the largest ones, up to a total of three lesions (malignant and benign combined). If there was no malignant lesion, benign lesions were pointed out, from the largest to the smallest, up to three lesions. In cases where local treatment was performed, local recurrence was classified as a malignant lesion and, in the absence of recurrence, the lesion was classified as benign.

Two certified radiologists (each with 10 years of experience) independently conducted the image interpretation experiments. The observers were provided the following information before interpretation: what kind of the underlying liver disease or presence of extrahepatic malignant tumor, and the history of therapy, for example, radiofrequency ablation or resection. This information is often provided in daily clinical work; hence, the effect of this information on the image interpretation would be minimum. First, the observers performed image interpretation with datasets lacking the perfusion study and indicated the liver lesion on the printed enhanced T2*-weighted images (the flip angle was 30°). Then, they classified the lesions into the following four categories: (I) no lesion; (II) benign lesion; (III) possible malignant lesion; (IV) definitive malignant lesion. In other words, category 1 indicates that the patient has no lesions. One month after the initial interpretation, the observers performed an interpretation study with a

full dataset that this time included a perfusion study. The radiological diagnostic criteria were based on the following possibilities: (I) hemangioma shows obvious hyperintensity on T2-weighted image and hyperintensity on enhanced T1-weighted image of short TE 3 min after SPIO injection (20); (II) cysts show obvious hyperintensity on T2-weighted images, no enhancement on enhanced T1-weighted image of short TE, and hyperintensity on apparent diffusion coefficient (ADC) map. The lesion showing intermediate hyperintensity on the T2-weighted image and restricted diffusion (hyperintensity on DWI and hypointensity on ADC map) was considered malignant (21,22). The post-therapeutic lesions that showed hyperintensity on the T2-weighted image, and iso- or hypointensity on the DWI, were considered to have no recurrence and in a good therapeutic course (23), and were eventually classified as a benign lesion. The decreasing signal intensity on the T2-weighted image due to SPIO accumulation was observed in well-differentiated HCC or focal nodular hyperplasia (FNH). The observers referred to the morphological findings, such as a central stellate scar or septal fibrosis, to distinguish HCC from FNH. A perfusion study was used to evaluate the lesion hemodynamics. If the arterial blood flow increased in the post-therapeutic lesion, the lesion was considered a recurrence, and the observers classified the lesion as malignant. If the lesion signal decreased, even in untreated lesions, indicating an increase in arterial blood flow in the perfusion study, and the lesion showed restricted diffusion on the DWI, it was diagnosed as malignant.

The side effect associated with SPIO was evaluated based on the medical record. The physical condition was certainly evaluated just after the MRI examination and around 1 week after this MRI exam. Regular hematology or urinalysis has not been done for this study.

Statistical analysis

Receiver operating characteristic (ROC) analysis was performed to evaluate the diagnostic performance of SPIO-enhanced MRI with or without a perfusion study. The diagnostic agreement of the observers was evaluated with a weighted kappa test. The agreement rates were defined as follows: $0 \leq rate \leq 0.4$, poor agreement; $0.4 < rate \leq 0.6$, moderate agreement; $0.6 < rate \leq 0.8$, good agreement; $0.8 < rate \leq 1.0$ excellent agreement.

Results

The records of 26 patients were evaluated, including eight patients with asthma, two patients with a history of side effects with Gd-based contrast media, 16 patients with renal dysfunction [five with G5, three with G4, five with G3b, and three with G3a with Kidney Disease Improving Global Outcomes (KDIGO) staging criteria for chronic kidney disease (CKD)] (24). None of these patients experienced any adverse effects associated with the use of SPIO (*Table 1*).

The final diagnoses were four liver metastatic nodules (one was proven by surgery, and three were confirmed by clinical course), 10 HCC nodules (four were proven by biopsy including three moderately differentiated and one well-differentiated, and six were confirmed by the clinical course), one FNH, 24 HCC post-treatment lesions (without recurrence), one meta-treatment lesion (without recurrence), and two were cysts; three patients had no lesion (*Table 1*). A representative case is shown in *Figure 2*.

Regarding the diagnostic performance of liver lesions, when the perfusion study was excluded from the evaluation, the area under the curve (Az) values were 0.473 (P=0.794, 95% CI: 0.275–0.672) and 0.602 (P=0.305, 95% CI: 0.407–0.798) for observers 1 and 2 (*Figure 3*). When the perfusion study was included in the evaluation, the Az values were 0.782 (P=0.011, 95% CI: 0.565–0.998) for observer 1 and 0.784 (P=0.004, 95% CI: 0.591–0.977) for observer 2 (*Figure 3*). These findings indicate that, for both observers, the confidence level significantly increased when the perfusion study was included (P=0.001 and 0.012 by observers 1 and 2). However, the agreement of the observer was moderate (k=0.419) when the perfusion study was not included in the assessment. The agreement decreased to k=0.340 when the perfusion study was included in the assessment, and it was a poor agreement.

Discussion

Although this study was based on a small number of cases, it has demonstrated the feasibility of SPIO-enhanced MRI in patients who are unable to undergo contrast-enhanced CT or contrast-enhanced MRI with Gd-based contrast media. Previous studies have reported that the Az value of dynamic CT for HCC was around 0.66–0.95 (7-9,25), while the metastatic tumor was around 0.69–0.93 (16,18,19,26). These results were dependent on the lesion size. This

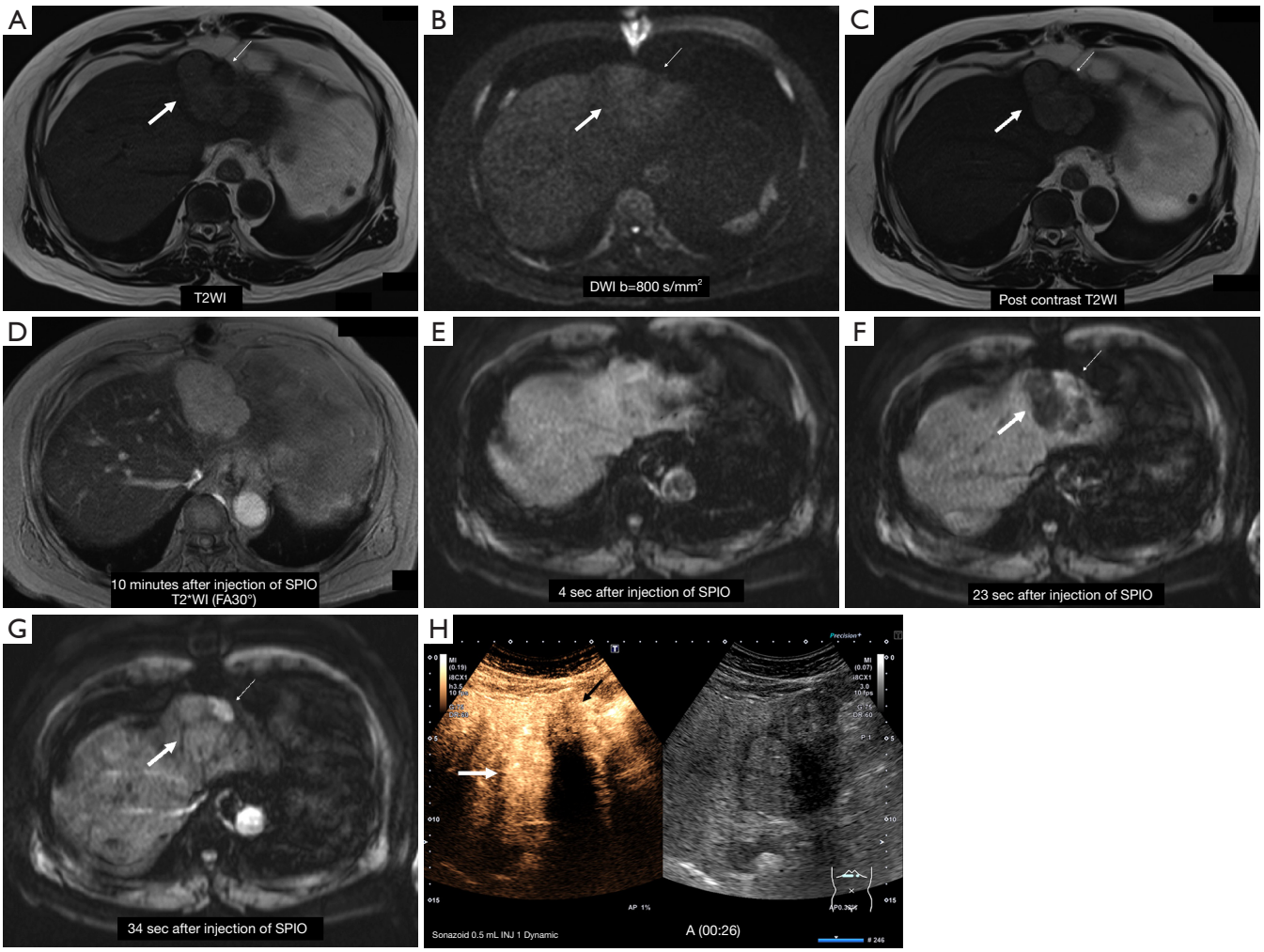

Figure 2 A 77-year-old man with HCC and renal dysfunction (Kidney Disease Improving Global Outcomes staging criteria for chronic kidney disease staging G4). The HCC located in the left lobe was treated with radiofrequency ablation. (A) T2-weighted image shows a slight hyperintense lesion on the left lateral lobe (large arrow). A small arrow indicates the ablated region. (B) HCC shows a slight hyperintense lesion on a DWI (large arrow). The ablated region shows hypo-intensity (small arrow). (C) The contrast between tumor and liver increased in the post-contrast-enhanced T2-weighted image compared to the pre-contrast-enhanced image (A). (D) The contrast between tumor and liver on the T2* weighted image was the highest among the acquired images. (E-G). These consecutive images are pre-contrast, 23 s, and 34 s after injection of SPIO in the perfusion study. The signal drop is seen at 23 s after injection of SPIO (large arrow). The ablated region shows no signal change (small arrow), indicating no recurrence. However, the signal of recurrence tumor shows a quick recovery at 34 s. (H) The contrast-enhanced US reveals that the tumor is hypervascular (white arrow), while the ablated region (black arrow) shows no enhancement. HCC, hepatocellular carcinoma; DWI, diffusion-weighted image; SPIO, superparamagnetic iron oxide.

study included HCC and metastatic tumors; moreover, the post locoregional therapeutic lesion was also included. Therefore, the diagnosis may be more difficult. Hence, we believe that the usefulness in patients who cannot use iodine contrast agents or hepatocyte-specific MR contrast agents, addressed in the present study, cannot be ignored.

While a limitation of SPIO-enhanced MRI is its inability to visualize tumor blood flow, the addition of a perfusion study increased diagnostic confidence for liver lesions, which is consistent with results previously reported for other imaging techniques (7-9,16,18,19,25,26). In this study, a substantial proportion of patients were evaluated

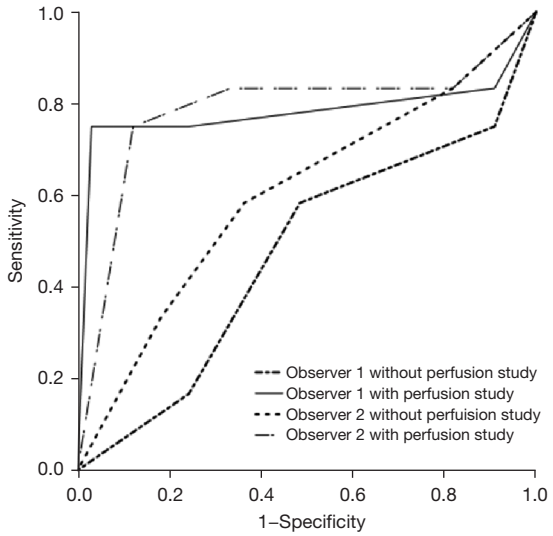

Figure 3 Receiver operating characteristic analysis curve showing the diagnostic performance of the SPIO-enhanced MRI for liver lesions. When the perfusion study was excluded from the evaluation, the Az values were 0.473 for observer 1 and 0.602 for observer 2. When the perfusion study was included in the evaluation, the Az values were 0.782 for observer 1 and 0.784 for observer 2. For both observers, the confidence level increased when the perfusion study was included. SPIO, superparamagnetic iron oxide.

for therapeutic results after locoregional treatment of HCC, which was thought to be due to the need to evaluate vascularity to assess local recurrence or residual tumor.

Although SPIO is excellent for tumor detection, it has limitations in assessing the residual arterial blood flow after locoregional therapy of liver tumors without perfusion studies. Therefore, tumor treatment efficacy has been judged by whether sufficiently ablated margins are obtained compared to the preoperative images or whether a restricted diffusion area suggests recurrence or residual tumor on the DWIs. If there is some viable component after transarterial chemoembolization (TACE), the lesion shows restricted diffusion (23). However, the efficacy of diffusion-weighted imaging for the presence of recurrence after RFA has not been established (27,28). Reports are showing that it is effective in HCC, while there are negative reports in metastatic tumors (29,30). In this study, only a qualitative evaluation was performed, and a quantitative evaluation, such as the measurement of ADC values, was not performed. However, since we could confirm the effectiveness of visual evaluation of arterial blood flow, thus, our findings show that adding a perfusion study to SPIO-enhanced MRI increases diagnostic performance to levels near those seen with iodine CT (7-9,16,18,19,25,26), suggesting that this approach is a reasonable alternative in patients with contraindications.

This study showed that SPIO could be safely used in patients with asthma, renal dysfunction, and a history of adverse effects from Gd–based contrast agents. In this study, SPIO was used in patients with eGFR <60 mL/min/1.73 m^2 instead of an iodine contrast medium. Although there is no consensus on using an iodine contrast medium for patients with renal dysfunction, it is accepted that patients with renal dysfunction with eGFR <30 mL/min/1.73 m^2 should be treated with prophylactic saline infusion (24). In patients undergoing chemotherapy, we should be cautious about contrast media administration, as it may be difficult to continue treatment due to the decreased renal function. In such cases, SPIO-enhanced MRI may be an option for patients who are hesitant to receive CT or Gd-based contrast media.

A limitation of this study is the small number of cases. We only included patients who could not tolerate contrast-enhanced CT or hepatocyte-specific MR contrast agents, which resulted in only a few cases. We believe that additional cases should be studied in the future. In addition, the perfusion study reported here is currently available for only six slices and does not cover the entire liver. Therefore, it is necessary to determine the imaging range in the pre-contrast examination. In this respect, there is a bias. In addition, for six of 51 nodules, the lesion to be evaluated was out of the imaging range due to inappropriate breath-holding, so we were unable to assess the performance of SPIO-enhance MRI for these nodules. In the future, it is expected that a sufficient number of examinations will increase the number of images available for analysis.

Conclusions

SPIO-enhanced MRI for liver lesion assessment was feasibly performed in patients with renal dysfunction, asthma, or a history of adverse effects to iodine contrast agents or Gd-based contrast media, thereby providing an alternative MRI approach for these patients. A perfusion study should be included in SPIO-enhanced MRI to detect the target lesion.

Acknowledgments

Funding: None.

Footnote

Reporting Checklist: The authors have completed the STROBE reporting checklist. Available at https://qims.amegroups.com/article/view/10.21037/qims-22-74/rc

Conflicts of Interest: All authors have completed the ICMJE uniform disclosure form (available at https://qims.amegroups.com/article/view/10.21037/qims-22-74/coif). Kazuhiro Saito reports personal fees from Bayer, grants and personal fees from Eisai, grants and personal fees from Daiichi Sankyo, grants and personal fees from FUJIFILM Toyama Chemical, personal fees from Siemens, grants and personal fees from Nihon Medi-Physics, outside the submitted work. Yoichi Araki reports personal fees from Siemens. The other authors have no conflicts of interest to declare.

Ethical Statement: The authors are accountable for all aspects of the work in ensuring that questions related to the accuracy or integrity of any part of the work are appropriately investigated and resolved. This study was conducted in accordance with the Declaration of Helsinki (as revised in 2013). The institutional ethics review board of Tokyo Medical University (No. T2020-0339) approved this retrospective case-control study and individual consent for this retrospective analysis was waived.

References

1. Ichikawa T, Saito K, Yoshioka N, Tanimoto A, Gokan T, Takehara Y, Kamura T, Gabata T, Murakami T, Ito K, Hirohashi S, Nishie A, Saito Y, Onaya H, Kuwatsuru R, Morimoto A, Ueda K, Kurauchi M, Breuer J. Detection and characterization of focal liver lesions: a Japanese phase III, multicenter comparison between gadoxetic acid disodium-enhanced magnetic resonance imaging and contrast-enhanced computed tomography predominantly in patients with hepatocellular carcinoma and chronic liver disease. Invest Radiol 2010;45:133-41.
2. Li J, Wang J, Lei L, Yuan G, He S. The diagnostic performance of gadoxetic acid disodium-enhanced magnetic resonance imaging and contrast-enhanced multi-detector computed tomography in detecting hepatocellular carcinoma: a meta-analysis of eight prospective studies. Eur Radiol 2019;29:6519-28.
3. Vreugdenburg TD, Ma N, Duncan JK, Riitano D, Cameron AL, Maddern GJ. Comparative diagnostic accuracy of hepatocyte-specific gadoxetic acid (Gd-EOB-DTPA) enhanced MR imaging and contrast enhanced CT for the detection of liver metastases: a systematic review and meta-analysis. Int J Colorectal Dis 2016;31:1739-49.
4. Huynh K, Baghdanian AH, Baghdanian AA, Sun DS, Kolli KP, Zagoria RJ. Updated guidelines for intravenous contrast use for CT and MRI. Emerg Radiol 2020;27:115-26.
5. Ahn YH, Kang DY, Park SB, Kim HH, Kim HJ, Park GY, Yoon SH, Choi YH, Lee SY, Kang HR. Allergic-like Hypersensitivity Reactions to Gadolinium-based Contrast Agents: An 8-year Cohort Study of 154 539 Patients. Radiology 2022;303:329-36.
6. Nelson KL, Gifford LM, Lauber-Huber C, Gross CA, Lasser TA. Clinical safety of gadopentetate dimeglumine. Radiology 1995;196:439-43.
7. Hori M, Murakami T, Kim T, Tsuda K, Takahashi S, Okada A, Takamura M, Nakamura H. Detection of hypervascular hepatocellular carcinoma: comparison of SPIO-enhanced MRI with dynamic helical CT. J Comput Assist Tomogr 2002;26:701-10.
8. Lee JM, Kim IH, Kwak HS, Youk JH, Han YM, Kim CS. Detection of small hypervascular hepatocellular carcinomas in cirrhotic patients: comparison of superparamagnetic iron oxide-enhanced MR imaging with dual-phase spiral CT. Korean J Radiol 2003;4:1-8.
9. Kim SH, Choi D, Kim SH, Lim JH, Lee WJ, Kim MJ, Lim HK, Lee SJ. Ferucarbotran-enhanced MRI versus triple-phase MDCT for the preoperative detection of hepatocellular carcinoma. AJR Am J Roentgenol 2005;184:1069-76.
10. Ward J, Robinson PJ, Guthrie JA, Downing S, Wilson D, Lodge JP, Prasad KR, Toogood GJ, Wyatt JI. Liver metastases in candidates for hepatic resection: comparison of helical CT and gadolinium- and SPIO-enhanced MR imaging. Radiology 2005;237:170-80.
11. Nishie A, Tajima T, Ishigami K, Ushijima Y, Okamoto D, Hirakawa M, Nishihara Y, Taketomi A, Hatakenaka M, Irie

H, Yoshimitsu K, Honda H. Detection of hepatocellular carcinoma (HCC) using super paramagnetic iron oxide (SPIO)-enhanced MRI: Added value of diffusion-weighted imaging (DWI). J Magn Reson Imaging 2010;31:373-82.
12. Imai Y, Murakami T, Yoshida S, Nishikawa M, Ohsawa M, Tokunaga K, Murata M, Shibata K, Zushi S, Kurokawa M, Yonezawa T, Kawata S, Takamura M, Nagano H, Sakon M, Monden M, Wakasa K, Nakamura H. Superparamagnetic iron oxide-enhanced magnetic resonance images of hepatocellular carcinoma: correlation with histological grading. Hepatology 2000;32:205-12.
13. Saito K, Shindo H, Ozuki T, Ishikawa A, Kotake F, Shimazaki Y, Abe K. Perfusion study of hypervascular hepatocellular carcinoma with SPIO. Magn Reson Med Sci 2005;4:151-8.
14. Saito K, Sugimoto K, Nishio R, Araki Y, Moriyasu F, Kakizaki D, Tokuuye K. Perfusion study of liver lesions with superparamagnetic iron oxide: distinguishing hepatocellular carcinoma from focal nodular hyperplasia. Clin Imaging 2009;33:447-53.
15. Saito K, Ledsam J, Sourbron S, Araki Y. Validation study of perfusion parameter in hypervascular hepatocellular carcinoma and focal nodular hyperplasia using dynamic susceptibility magnetic resonance imaging with superparamagnetic iron oxide: comparison with single level dynamic CT arteriography. Quant Imaging Med Surg 2020;10:1298-306.
16. Kim YK, Ko SW, Hwang SB, Kim CS, Yu HC. Detection and characterization of liver metastases: 16-slice multidetector computed tomography versus superparamagnetic iron oxide-enhanced magnetic resonance imaging. Eur Radiol 2006;16:1337-45.
17. Mainenti PP, Mancini M, Mainolfi C, Camera L, Maurea S, Manchia A, Tanga M, Persico F, Addeo P, D'Antonio D, Speranza A, Bucci L, Persico G, Pace L, Salvatore M. Detection of colo-rectal liver metastases: prospective comparison of contrast enhanced US, multidetector CT, PET/CT, and 1.5 Tesla MR with extracellular and reticulo-endothelial cell specific contrast agents. Abdom Imaging 2010;35:511-21.
18. Motosugi U, Ichikawa T, Nakajima H, Sou H, Sano M, Sano K, Araki T, Iino H, Fujii H, Nakazawa T. Imaging of small hepatic metastases of colorectal carcinoma: how to use superparamagnetic iron oxide-enhanced magnetic resonance imaging in the multidetector-row computed tomography age? J Comput Assist Tomogr 2009;33:266-72.
19. Muhi A, Ichikawa T, Motosugi U, Sou H, Nakajima H, Sano K, Kitamura T, Faima Z, Fukushima K, Araki T, Iino H, Mori Y, Fujii H. Diagnosis of colorectal hepatic metastases: Contrast-enhanced ultrasonography versus contrast-enhanced computed tomography versus superparamagnetic iron oxide-enhanced magnetic resonance imaging with diffusion-weighted imaging. J Magn Reson Imaging 2010;32:1132-40.
20. Kim JH, Kim MJ, Suh SH, Chung JJ, Yoo HS, Lee JT. Characterization of focal hepatic lesions with ferumoxides-enhanced MR imaging: utility of T1-weighted spoiled gradient recalled echo images using different echo times. J Magn Reson Imaging 2002;15:573-83.
21. Colagrande S, Castellani A, Nardi C, Lorini C, Calistri L, Filippone A. The role of diffusion-weighted imaging in the detection of hepatic metastases from colorectal cancer: A comparison with unenhanced and Gd-EOB-DTPA enhanced MRI. Eur J Radiol 2016;85:1027-34.
22. Han S, Choi JI, Park MY, Choi MH, Rha SE, Lee YJ. The Diagnostic Performance of Liver MRI without Intravenous Contrast for Detecting Hepatocellular Carcinoma: A Case-Controlled Feasibility Study. Korean J Radiol 2018;19:568-77.
23. Liu Z, Fan JM, He C, Li ZF, Xu YS, Li Z, Liu HF, Lei JQ. Utility of diffusion weighted imaging with the quantitative apparent diffusion coefficient in diagnosing residual or recurrent hepatocellular carcinoma after transarterial chemoembolization: a meta-analysis. Cancer Imaging 2020;20:3.
24. Davenport MS, Perazella MA, Yee J, Dillman JR, Fine D, McDonald RJ, Rodby RA, Wang CL, Weinreb JC. Use of Intravenous Iodinated Contrast Media in Patients with Kidney Disease: Consensus Statements from the American College of Radiology and the National Kidney Foundation. Radiology 2020;294:660-8.
25. Kim YK, Kwak HS, Kim CS, Chung GH, Han YM, Lee JM. Hepatocellular carcinoma in patients with chronic liver disease: comparison of SPIO-enhanced MR imaging and 16-detector row CT. Radiology 2006;238:531-41.
26. Onishi H, Murakami T, Kim T, Hori M, Iannaccone R, Kuwabara M, Abe H, Nakata S, Osuga K, Tomoda K, Passariello R, Nakamura H. Hepatic metastases: detection with multi-detector row CT, SPIO-enhanced MR imaging, and both techniques combined. Radiology 2006;239:131-8.
27. Lu TL, Becce F, Bize P, Denys A, Meuli R, Schmidt S. Assessment of liver tumor response by high-field (3 T) MRI after radiofrequency ablation: short- and mid-term evolution of diffusion parameters within the ablation zone. Eur J Radiol 2012;81:e944-50.

28. Yuan ZG, Wang ZY, Xia MY, Li FZ, Li Y, Shen Z, Wang XZ. Comparison of diffusion kurtosis imaging versus diffusion weighted imaging in predicting the recurrence of early stage single nodules of hepatocellular carcinoma treated by radiofrequency ablation. Cancer Imaging 2019;19:30.
29. Barat M, Fohlen A, Cassinotto C, Jannot AS, Dautry R, Pelage JP, Boudiaf M, Pocard M, Eveno C, Taouli B, Soyer P, Dohan A. One-month apparent diffusion coefficient correlates with response to radiofrequency ablation of hepatocellular carcinoma. J Magn Reson Imaging 2017;45:1648-58.
30. Gordic S, Corcuera-Solano I, Stueck A, Besa C, Argiriadi P, Guniganti P, King M, Kihira S, Babb J, Thung S, Taouli B. Evaluation of HCC response to locoregional therapy: Validation of MRI-based response criteria versus explant pathology. J Hepatol 2017;67:1213-21.

Cite this article as: Kurata C, Saito K, Shirota N, Araki Y, Sugimoto K, Tajima Y, Yunaiyama D. The feasibility of superparamagnetic iron oxide–enhanced magnetic resonance imaging for assessing liver lesions in patients with contraindications for iodine CT contrast media or gadolinium-based MR contrast media: a retrospective case-control study. Quant Imaging Med Surg 2022;12(9):4612-4621. doi: 10.21037/qims-22-74

